EPJ manuscript No.
(will be inserted by the editor)

Structure and dynamics of high and low density water molecules in the liquid and supercooled regimes

Joan Manuel Montes de Oca[1], J. Ariel Rodriguez Fris[1], Sebastián R. Accordino[1], David C. Malaspina[2] and Gustavo A. Appignanesi[1]

[1] Sección Fisicoquímica - INQUISUR and Departamento de Química, Universidad Nacional del Sur, Avenida Alem 1253, 8000-Bahía Blanca, Argentina.
[2] Northwestern University, USA.

Received: date / Revised version: date

Abstract. By combining the local structure index with potential energy minimisations we study the local environment of the water molecules for a couple of water models, TIP5P-Ew and SPC/E, in order to characterise low and high density "species". Both models show a similar behaviour within the supercooled regime, with two clearly distinguishable populations of unstructured and structured molecules, the fraction of the latter increasing with supercooling. Additionally, for TIP5P-Ew, we find that the structured component vanishes quickly at the normal liquid regime (above the melting temperature). Thus, while SPC/E provides a fraction of structured molecules similar to that found in X-ray experiments, we show that TIP5P-Ew underestimates such value. Moreover, unlike SPC/E, we demonstrate that TIP5-Ew does not follow the linear dependence of the logarithm of the structured fraction with inverse temperature, as predicted by the two-order parameter model. Finally, we link structure to dynamics by showing that there exists a strong correlation between structural fluctuation and dynamics in the supercooled state with spatial correlations in both static and dynamic quantities.

PACS. 61.20.Ja Computer simulation of liquid structure – 61.25.Em Molecular liquids

1 Introduction

Even when water is one of the most abundant molecules on earth and is essential for main contexts spreading from materials science to biology, the comprehension of its structure and behaviour is still far from being complete [1–12]. In particular, liquid water presents an unusual amount of anomalies [8–11] stemming from the existence of two competing preferential local structures identified with molecules characterised by high- or low-local density [9,13–20]. This description was inspired by the coexistence of two different forms of amorphous glasses: low-density amorphous ice LDA and high-density amorphous ice HDA [21,22]. Thus, it is expected that, in the liquid regime, water consists of a mixture of two kinds "species": low local density, well structured LDA-like molecules and high local density, unstructured HDA-like ones. Several indices [23–26,13,14] have thus been developed to identify structured and unstructured molecules. One of such indicators is the local structure index, I [13,14], which is sensitive to the presence or absence of a gap between the first and second coordination shells in liquid water. This index has recently regained considerable attention since we have shown that, when combined with local minimisations of potential energy, that is, when applied to the so-called inherent structures, IS (an IS being the local basin of attraction of the actual configuration in the potential energy surface), it is able to produce a clear bimodal distribution of structured and unstructured molecules both for the supercooled and normal liquid regimes [20]. We note that this bimodal behaviour that enables an easy determination of locally "well-structured" and "unstructured" water molecules, is not present in the real dynamics (the actual runs, without minimisation). By quantifying the fraction of structured molecules as a function of temperature [27] we have corroborated the predictions of the proposed two-order-parameter model of water [17–19] showing that such fraction can indeed be described by a Boltzmann factor where the Boltzmann weight expresses the stabilisation due to the hydrogen bond energy of the locally favored well-developed hydrogen bonds structure and the destabilisation, proportional to the pressure, stemming from the concurrent volume increase [27,17–19]. The I/inherent structures approach has been applied for different water models (like SPC/E [20,27], TIP4P-ice [28] and TIP4P/2005 [29] showing in all cases a clear bimodal distribution with a temperature-independent (isosbestic-like) minimum. More recently, the group of Roberto Car [31] has confirmed this scenario for the more sophisticated ab initio potentials within the framework of density functional theory.

In turn, concerning dynamics, the structural (or α) relaxation of supercooled and liquid water has been shown to be due to the occurrence of dynamical events characterised by relatively compact clusters (d-clusters) of fast moving molecules that develop intermittently in bursts of mobility [32]. This behaviour is equivalent to that found computationally for other systems like binary Lennard-Jones glasses [33] and liquid silica [34] and experimentally in single-molecule experiments in polymeric systems [35]) and colloidal suspensions [36].

Within this context, the aim of the present work is to study the local structure of high and low density water molecules both in the TIP5P-Ew and SPC/E models of water. We shall find that TIP5P-Ew only displays a measurable population of structured molecules below the melting temperature, while SPC/E and other studied models yield a significant amount even at ambient temperature. Additionally, we also study the structural details of the local order of the high and low local density molecules together with their temperature evolution to find results that are in accord with the two-order parameter model. Finally, we also link structure to dynamics by relating structural changes to relaxation events.

2 Discriminating structured and unstructured molecules

This section is devoted to determine structured and unstructured molecules [20]. We study the behaviour of two water models: TIP5P-Ew and SPC/E. In the first case we used NpT ensemble of 512 water molecules at 1 atm [38]. In the second case we conduct NVE molecular dynamics simulations of a system of 216 water molecules [37]. In both cases we used periodic boundaries. To quantify the local order of the water molecules Shiratani and Sasai [13,14] proposed the local structure index I. This indicator stems from the observation of the existence of certain molecules which show an unoccupied gap between 3.2 Å and 3.8 Å in their radial neighbour distribution. Such low-density molecules are well structured and coordinated in a highly tetrahedral manner with other four water molecules. In turn, other water molecules display occupancy of such gap, a fact that increases the local density and distorts the tetrahedral order of the central molecule. To compute $I(i,t)$ for molecule i at time t, one orders the rest of the molecules depending on the radial distance r_j between the oxygen of the molecule i and the oxygen of molecule j : $r_1 < r_2 < r_j < r_{j+1} < \ldots < r_{n(i,t)} < r_{n(i,t)+1}$, where $n(i,t)$ is chosen so that $r_{n(i,t)} < 3.7\,\text{Å} < r_{n(i,t)+1}$. Then, $I(i,t)$ is calculated as follows:

$$I(i,t) = \frac{1}{n(i,t)} \sum_{j=1}^{n(i,t)} [\Delta(j;i,t) - \overline{\Delta}(i,t)]^2$$

where $\Delta(j;i,t) = r_{j+1} - r_j$ and $\overline{\Delta}(i,t)$ is the average over all molecules of $\Delta(j;i,t)$. Thus, $I(i,t)$ expresses the inhomogeneity in the radial distribution within the sphere of radius around 3.7 Å. A high value of $I(i,t)$ implies that molecule i at time t is characterised by a tetrahedral local order and a low-local density, while on the contrary, values of $I(i,t) \sim 0$ indicate a molecule with defective tetrahedral order and high-local density. Differently from Refs. [13,14] we calculate such index in the inherent structures IS (minimising the potential energy of the corresponding instantaneous structure) to filter out the randomizing effect introduced by the thermal vibrations [39], effectively removing the fluctuations present in the real trajectory which hamper the possibility of properly identifying the local structure.

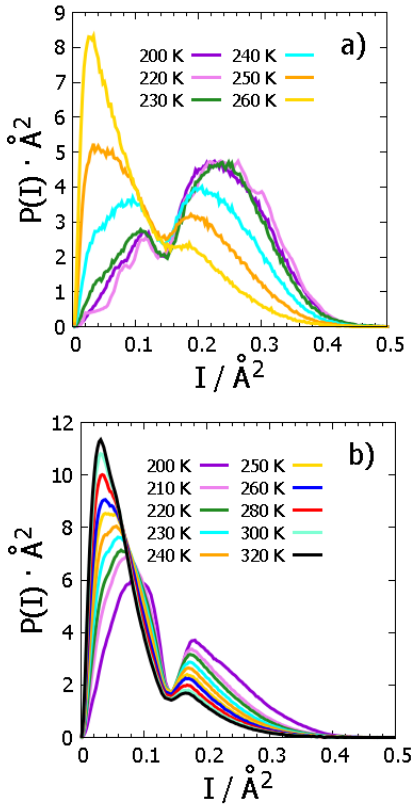

Fig. 1. Probability density $P(I)$ of finding a water molecule with local structure index I for a range of temperatures within the normal and supercooled liquid regimes in the inherent dynamics for density 1 g/mL. a) TIP5P-Ew, b) SPC/E.

Figures 1 show the distribution of $I(i,t)$ for a range of temperatures for the two models studied, TIP5P-Ew and SPC/E, whose melting temperatures have been estimated to be respectively $T = 271$ K and $T = 214$ K [40]. In both cases, we find clear bimodal distributions in the inherent dynamics regime. The left peak (whose amplitude decreases as T decreases) signals the presence of unstructured (high-density) water molecules, while the right peak (whose amplitude increases as T decreases) is indicative of highly structured (low-density) molecules. The minimum that separates both peaks is invariant for all studied temperatures (a kind of "isosbestic point") and is located at $I_{\min} \sim 0.14$ Å^2 for both water models. This result

points to the existence of two populations with well characterised local structures in dynamical equilibrium and whose relative concentration changes with T. A notable exception is the order parameter proposed by Russo and Tanaka [41] which shows bimodal features for different water models without energy minimization. However, we here find an interesting difference between the two models studied. For the SPC/E model the bimodality is not only evident within the supercooled regime but extends significantly into the normal liquid regime (even when the structured component or right peak decreases as T increases). This has also been found for other water models like TIP4P/2005 [29], where a relative population of unstructured to structured molecules of 3:1 at ambient temperature has been determined in agreement with X-ray insights [29]. Instead, from Fig. 1a we can learn that the data for the TIP5P-Ew model display an evident bimodal distribution in the supercooled regime while the bimodality distribution tends to fade at temperatures close to the melting point since the fraction of the structured molecules drops significantly. Such a difference between the behaviour of SPC/E and TIP5P-Ew models as evidenced by Figs. 1 is intriguing. TIP5P-Ew has been developed to favor local tetrahedral order but presents a melting temperature close to the experimental value ($T = 271$ K [40]), while SPC/E has a much lower melting point ($T = 214$ K [40]). The effect could be due to certain failures of TIP5P-Ew in describing water structure at higher T, as has been already pointed out [30]. For SPC/E the right peak that signals the structured state is sharp and its position (around $I = 0.175$ Å^2) is insensitive to temperature. This behaviour is almost identical to what is found for other water models like TIP4P/2005 [29], TIP4P-ice [28,31] and ab initio models [31], and is expected in terms of the two-order parameter model [17–19] that proposes that the structured state is given by a single or a few similar structures. For TIP5P-Ew, however, this peak is much broader and, as T decreases, notably moves to the right, even reaching values much larger than 0.2 Å^2. This fact is consistent with a structured state made of a variety of different well-structured molecules, at odds with the proposal of the two-order parameter model.

3 Details of the local environment of structured and unstructured molecules

The central observation of Shiratani and Sasai that leads to the development of I was based on the fact that well structured molecules present a clear separation between the first and the second coordination shells that enables the first one to be well tetrahedrally coordinated, while for unstructured molecules neighbour from the second shell (mainly the fifth neighbour) intrude this gap perturbing the tetrahedral order of the first shell. Thus, well structured molecules present a low local density while unstructured molecules display a high local density. In order to learn on the details of the local environment of structured and unstructured molecules we have classified water molecules by their I in ten different classes for the two water models studied. Figure 2a shows the oxygen-oxygen radial distribution function $g(r)$ for each class. As expected, in both models we obtain the typical first an second peaks. The molecules with I values from the highest ones up to that with values in the region of the minimum of the I distribution (I between 0.12 Å^2 and 0.16 Å^2) present a strict gap between the two peaks. However, for low-I molecules the existence of population in such region is evident. In fact, for the high-I molecules, as the I value decreases we find a shoulder preceding the second peak whose location moves to lower distances. However, in all cases no population is found around $r = 3.5$ Å, that is, in the gap region. In turn, for molecules with I lower than the minimum in the distribution $I_{\min}$, this shoulder is no more constrained to the region $r > 3.5$ Å but the whole region of $3.0 < r/\text{Å} < 3.5$ becomes populated. Water molecules at this region, or interstitial molecules, might be able to form elongated (low-energy) hydrogen bonds with the central molecule. In such case, these molecules could form the so-called bifurcated hydrogen bonds, a feature that has been shown to promote local mobility [47]. In fact we have found that geometrical arrangements (O-O distance lower than 3.6 Å and O...H-O angle larger than 110°) for this kind of defect are frequent for low-I molecules while they are not mainly found for high-I molecules. In the case of TIP5P-Ew and for 250 K we find for low-I and for high-I molecules, 1 % and 16 % with geometries compatible with bifurcated hydrogen bonds respectively. For SPC/E and 210 K the percentages are 3 and 60, respectively. In reference [27] we have studied the quality of hydrogen bonding parameters (normal or non-bifurcated hydrogen bonds) for structured and unstructured molecules finding O-O distances below 2.8 Å and O...H-O angles larger than 165° (we must bear in mind that we are using the inherent structure approach which improves the local structure of the molecules).

In Fig. 3 we show the distribution of distances r of the fifth neighbour to the central molecule for the different classes in which we divided the I values. We can see that both for TIP5P-Ew and SPC/E water models only for the low-I value molecules the fifth neighbour displays probability below $r = 3.5$ Å. In all cases, the peaks correspond to the shoulders of the radial distribution function of Fig. 2. Hence, for the high-I molecules, the fifth neighbour is clearly confined to the second shell thus preventing the disruption of the order of the first shell that would happen upon its intrusion in the inter-peak gap region, as evidently occurs for the low-I molecules. This fact is immediately evident from Fig. 4 where we display the probability distribution of distances r to the fourth neighbour for molecules with different I-values. These Figures show that for the high-I molecules the fourth neighbours are strictly confined to the region of the first-shell peak of the radial distribution function $g(r)$. However, the molecules within $I_{\min}$ display a splitting or broadening of such peak and a large tail. In turn, the low-I molecules present much broader distributions with a high probability beyond the $g(r)$-first-peak region. These results indicate

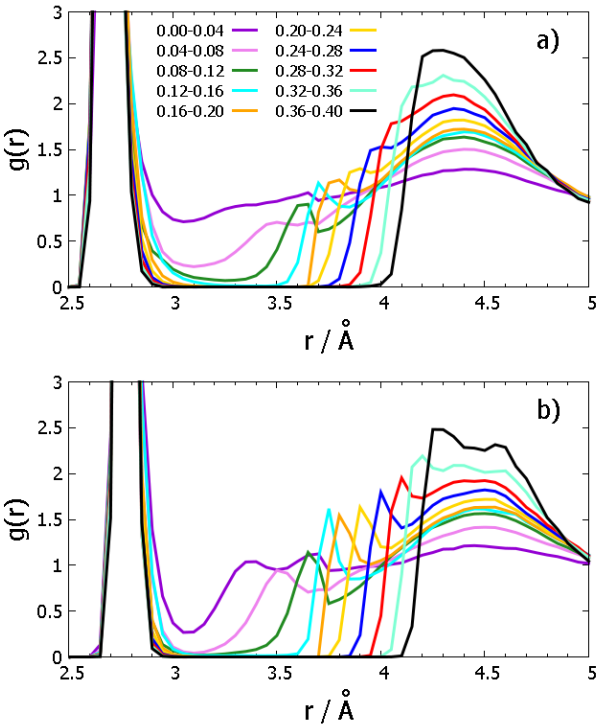

Fig. 2. Oxygen-oxygen radial distribution function $g(r)$ for water molecules classified according to their I value for a) TIP5P-Ew model at $T = 250$ K and for b) SPC/E model at $T = 210$ K. The range of I values in a) is in Å^2 and corresponds also for b).

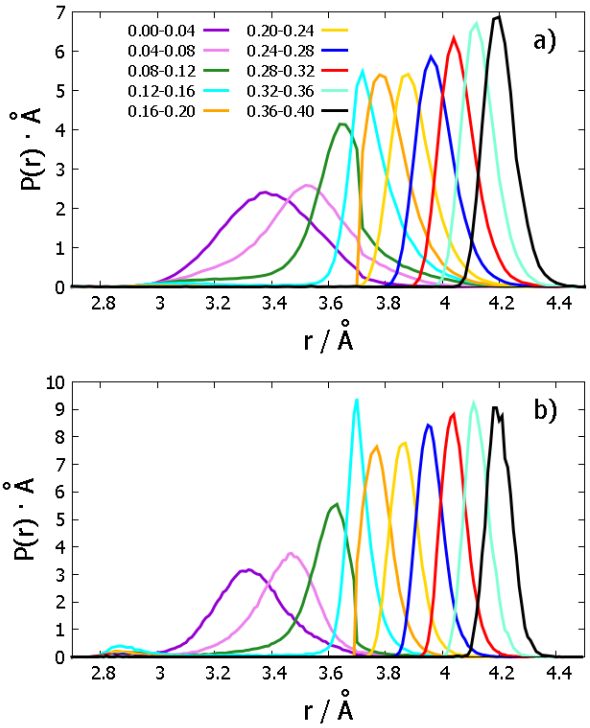

Fig. 3. Probability density $P(r)$ of finding a fifth neighbour at distance r, for water molecules classified according to their I values for a) TIP5P-Ew model at $T = 250$ K and for b) SPC/E model at $T = 210$ K. The range of I values in a) is in Å^2 and corresponds also for b).

that the structured molecules present an almost perfect first coordination shell clearly separated by a gap from the second shell while the order of the first shell of the unstructured molecules is spoiled by the intrusion of the fifth neighbours towards the inter-peak region.

4 Temperature dependence of the local structure index

As already illustrated by Fig. 1, the I distribution at the inherent dynamics presents a kind of isobestic (T-independent) minimum separating the structured and unstructured peaks. Additionally, the population of the structured molecules decreases at the expense of the unstructured component as T increases. Thus, in this section we shall focus on the T behaviour of the most representative or archetypical molecules of each class: "structured" (high I), "unstructured" (low I) and "isosbestic-point" $I_{\rm min}$ configurations. To this end, we shall identify the molecules that lie respectively within ± 0.01 Å^2 the maximum of the right peak (at position $I_{\rm right}$), the maximum of the left peak (at position $I_{\rm left}$) and the minimum of the distribution (at position $I_{\rm min}$) at the corresponding T. Then we build the $g(r)$ for each class of molecules and display the results in Figs. 5. From such a plot we can learn that, for SPC/E, the local order of the molecules within $I_{\rm right}$ and $I_{\rm min}$ are roughly insensitive to T. However, the situation is completely different for molecules within $I_{\rm left}$: while the positions of the peaks of the first and second coordination shell remain unchanged, as T increases we observe an increasing population in the region between these two peaks (a region that remains empty for both the molecules within $I_{\rm right}$ and $I_{\rm min}$). In fact, the development of a peak that at the highest T lies below $r > 3.5$ Å and moves towards the position of the first coordination shell as T increases is evident. Concurrently, the height of the second coordination shell peak lowers. Thus, as T increases the unstructured state is represented by locally more disordered configurations since the interstitial molecules (fifth neighbours) intrude more deeply into the gap region to produce more notable distortions in the tetrahedrality of the first coordination shell. This T-behaviour of the structured and unstructured component is again consistent with the picture put forth by the two-order-parameter model of water [17–19] where the structured state is expected to represent a rather unique (or a small number of closely-related) structures while the unstructured state would be made of a plethora of different structures or high entropy state.

For the case of TIP5P-Ew (Fig. 5b), the situation is similar in which concerns the left peak and the minimum. However, the behaviour is different for the case of the right peak. The $g(r)$ clearly depends on T in this case. Thus, the structure of the most representative molecules of the

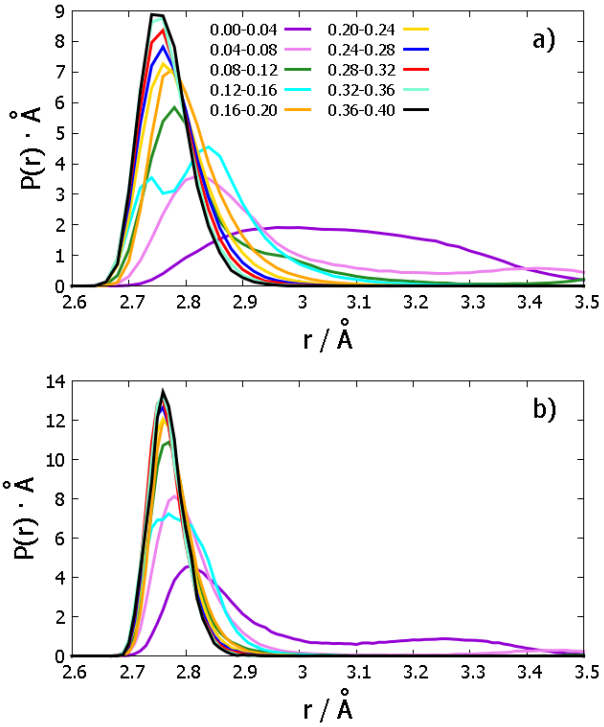

Fig. 4. Probability density $P(r)$ of finding a fourth neighbour at distance r, for water molecules classified according to their I values for a) TIP5P-Ew model at $T = 250$ K and for b) SPC/E model at $T = 210$ K. The range of I values in a) is in Å^2 and corresponds also for b).

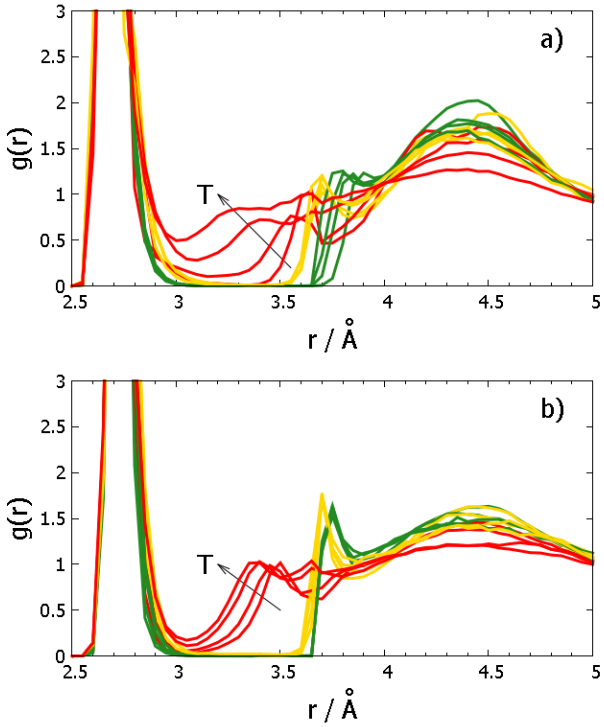

Fig. 5. Oxygen-oxygen radial distribution function $g(r)$ for molecules around the maximum of the high peak in the I-distribution ($I_{\text{right}} \pm 0.01$ Å^2) in green, around the maximum in the low I peak ($I_{\text{left}} \pm 0.01$ Å^2) in red, and around the minimum or isosbestic point ($I_{\text{min}} \pm 0.01$ Å^2) in yellow, as a function of T for a) TIP5P-Ew model (for 220 K, 240 K 250 K and 260 K) and for b) SPC/E model (for 210 K, 230 K, 260 K and 280 K).

structured state change with T, a fact that would not be reconciled with the expectations of the two-order parameter model.

5 Temperature dependence of the fraction of structured molecules

In this section we study the T dependence of the fraction of structured molecules ξ. This fraction is estimated by integrating the corresponding distribution of the local structure index $P(I)$ from I_{min} to the right. The results for TIP5P-Ew and SPC/E are displayed in Fig. 6. These results can be compared with the expectation of the two-order parameter model proposed by Tanaka [17–19]. This model regards water as a mixture of a few structured locally-favoured molecular arrangements and an unstructured liquid-like state comprising many different local configurations or high-entropy state, a proposition that differentiates from other two-state models of water like the mixture model [42–46]. Tanaka's model implies that the structured fraction ξ is governed by a Boltzmann weight proportional to the stabilization gained in improving the local structure (hydrogen bond energy) and to the destabilization, proportional to the pressure, stemming from the concurrent volume increase. Thus, ξ would display an exponential dependence on the reciprocal absolute T. In Fig. 6 we show the results (we plot in terms of a relative temperature, $1/T_{\text{r}}$, where $T_{\text{r}} = T/T_{\text{m}}$ and T_{m} is the melting temperature, in order to better compare the behaviour of TIP5P-Ew with SPC/E; the results for SPC/E are the same as in a work from our group [27]). We can see that SPC/E nicely follows the expected linear behaviour while this is clearly not the case for TIP5P-Ew. Additionally, TIP5P-Ew, as already indicated from the behaviour of the I-distributions, underestimates ξ at high temperatures (low values of $1/T_{\text{r}}$, above the melting point). That is, for the high T regime we can see that ξ for TIP5P-Ew is always well below the one estimated in the SPC/E model. Since TIP5P-Ew gives the correct value for the melting temperature, $1/T_{\text{r}}$ around 0.9 would represent ambient temperature. We can see that at $1/T_{\text{r}} = 0.9$, the SPC/E model yields a relation close to 3:1 of unstructured to structured molecules (that is, ξ is close to 0.25) a result consistent with previous findings both in the TIP4P/2005 model and in X-ray experiments [29]. However, for TIP5P-Ew, ξ is only around 0.15.

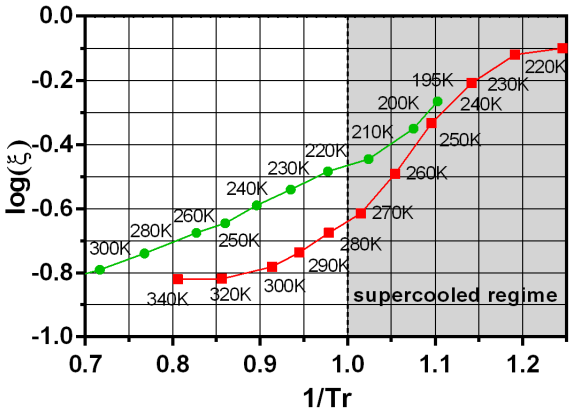

Fig. 6. Logarithm of the fraction of the structured molecules ξ as a function of the reciprocal reduced temperature $1/T_{\rm r} = T_{\rm m}/T$ ($T_{\rm m}$ being the melting temperature) for TIP5P-Ew (red) and SPC/E (green.)

6 Linking high and low I interchanges to glassy relaxation

As evident from the I distribution for the different T studied, the fraction of the structured component ξ increases at the expense of the unstructured one as T lowers. The high I or structured molecules present a better ice-like tetrahedral order while the unstructured ones exhibit a more disordered coordination. The unstructured state also presents the possibility to form bifurcated hydrogen bonds which lower the cost to rearrange the local hydrogen bond network given the fact that no net hydrogen bond breakage is demanded since one of the bifurcated bonds forms as the other one loosens and ultimately breaks (thus lowering the energy barrier). Additionally, there exist a great availability of different distorted configurations (that thus conform the high-entropy unstructured state), at variance from the more restricted set of structured configurations. Thus, the decrease in the population of unstructured molecules makes the relaxation dynamics to slow down.

In turn, the dynamics of glass-forming supercooled liquids have shown to present dynamical heterogeneities [49–51], that is, significant variations in the mobility of different spatial regions of the system that dramatically slow down the dynamics as the system is supercooled below its melting temperature. The structural relaxation is characterised by a timescale named as the α-relaxation time, τ_α, which quickly increases with the supercooling [49–51, 33,52,34]. Within this context we have shown by means of computer simulations for different glass-forming systems [33,52,34] including supercooled water [32], and by the analysis of experimental data in glass-forming systems [36], that the α-relaxation occurs by means of rapid cooperatively relaxing events which drive the system from one metabasin MB (group of similar structures) to another [56,33]. The MBs represent regions of the potential energy landscape PEL where the system is confined for long times. The mean lifetime of the confining MBs grows quickly as T is lowered in the supercooled regime. However, connections between static and dynamic properties in glass-forming liquids have been elusive, despite the significant amount of work devoted to this topic [53–55, 52]. However, some indicators have indeed been successful, like parameters based on locally favoured structures [57,41]. Thus, this section is aimed at finding connections between the time evolution of I changes and relaxation dynamics.

The relaxation dynamics of supercooled water can be monitored by the behaviour of the so-called distance matrix $\Delta^2(t',t'')$ [58,33]:

$$\Delta^2(t',t'') = N^{-1}\sum_{i=1}^{N}|\mathbf{r}_i(t') - \mathbf{r}_i(t'')|^2.$$

where $\mathbf{r}_i(t)$ is the position of the oxygen of molecule i at time t (in the inherent structure; but similar results are obtained if we instead use the real dynamics). Therefore, $\Delta^2(t',t'')$ gives the system averaged squared displacement of a molecule in the time interval that starts at t' and ends at t''. In other words, this distance matrix contains the averaged squared distances between (the oxygens of) each recorded structure and all the other ones. The first row of such matrix represents the squared displacement of the system from the original structure, that is, that at time $t = 0$. Figure 7a shows the distance matrix for a typical run in the SPC/E model, where the dark-squared islands (MB of the PEL [33,36,56]) indicate that the system is exploring similar structures, jumping from one MB to the next within a time much shorter than the time spent in each MB. Thus, the system is confined to a given region of its PEL for long times until a burst of mobility drives it to another region of the PEL. The confining times greatly increase as the system is supercooled thus producing the typical glassy slowing down. On the contrary, as T increases, the island structure begins to disappear and is completely lost at temperatures higher than the melting temperature.

In turn, in Figure 7b we show the structural Hamming distance matrix between the same structures used to calculate $\Delta^2(t',t'')$. For this matrix we classify the molecules of each structure either as low I index (unstructured) molecules or high I index (structured) molecules, provided I is respectively lower or higher than the minimum in the I distribution ($I_{\rm min}$, that is, the position of the isosbestic point). Thus, the Hamming distance $H(t',t'')$ between any pair of configurations t' and t'' is given by the number of molecules that reside in a different structural state in each configuration. Should the structural relaxation be unrelated to the dynamical changes that drive the glassy relaxation, we would find a different structural matrix pattern. For instance, if the structured and unstructured regions relaxed faster than the MB lifetimes, we would find a gradual shading in the Hamming distance matrix (that is, no island structure). On the contrary, the great similarity between the island-like objects displayed by Figures 7)a and b (exactly the same island positions), speaks of a

strong correlation between structural fluctuations and dynamics in the supercooled state with spatial correlations in both static and dynamic quantities. The cross correlation function between $\Delta^2(t',t'')$ and $H(t',t'')$ is $R \approx 0.6$ (this value is significant since a value close to zero would mean no correlation while $R = 1$ would indicate perfect correlation and $R = -1$ complete anti correlation). Thus, even when the molecules might change their local order frequently (for example, the unstructured molecules could explore different locally distorted configurations) the overall changes between structured and unstructured patterns must wait for the system to undergo the burst in mobility that drive the glassy relaxation. We note that here we only provide a temporal study of structured and unstructured regions, while we do not considered explicitly their spatial correlation. Such kind of study has been performed in references [29,59]. Finally, we do not find any preference in changes from structured to unstructured molecules or vice-versa in order to perform the islands transitions in $H(t',t'')$.

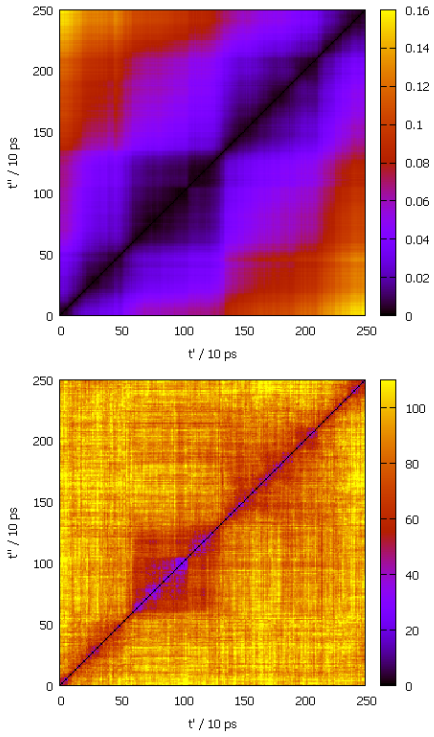

Fig. 7. a) Distance matrix $\Delta^2(t',t'')$ for a typical run for $T = 210$ K for the SPC/E model, units in legend are Å^2; b) Hamming matrix $H(t',t'')$ for the same run.

7 Conclusions

In this work we have studied the details of the local environment of the structured and unstructured water molecules for TIP5P-Ew and SPC/E water models. In the supercooled regime the behaviour for both models is qualitatively similar and consistent with the picture that also emerges for other models like TIP4P/2005 and TIP4P-ice and also for ab initio models based on the density functional formalism. However, within the normal liquid regime (above the melting temperature) the structured component is quickly lost with increasing temperature for TIP5P-Ew. We also studied the temperature dependence of the local structure order of the representative arrangements of the structured and unstructured states. Thus, for SPC/E we determined that the structured component is rather unique and insensitive to temperature, while the unstructured component corresponds to a broad group of different distorted configurations or high entropy state, as predicted by the two-order parameter model. In turn, TIP5P-Ew presents a broader high local-structure-order peak whose position depends on temperature, thus suggesting that the structured state would be made of a variety of many different local structures, a situation different from that expected from the two-order parameter model. Additionally, we have also studied the temperature dependence of the fraction of structured molecules. While SPC/E follows the prescription of the two-order parameter model, the non-linear behaviour of Fig. 6 shows that TIP5P-Ew clearly deviates from it. TIP5P-Ew also underestimates the fraction of structured molecules at high temperature (at variance from SPC/E and other models that yield results close to X-ray data). Finally, we demonstrated that while the unstructured molecules might explore different local arrangements in time within the supercooled regime, the patterns of structured and unstructured molecules require large bursts of mobility to decorrelate. Such events are precisely the ones that drive the α relaxation, thus connecting glassy dynamics to structural fluctuations.

Acknowledgments

Financial support from MinCyT and CONICET is gratefully acknowledged. GAA and JARF are research fellows of CONICET. SRA and JMMO thank CONICET for a fellowship.

References

1. D. M. Huang, D. Chandler, Proc. Natl. Acad. Sci. U.S.A. **97** 8324 (2000).
2. X. Huang, C. J. Margulis and B. J. Berne, Proc. Natl. Acad. Sci. U.S.A. **100** 11953 (2003).
3. A. Bizzarri and S. Cannistraro, J. Phys. Chem. B **106** 6617 (2002).
4. D. Vitkup, D. Ringe, G. A. Petsko and M. Karplus, Nat. Struct. Biol. **7** 34 (2000).
5. N. Choudhury and B. Montgomery Pettitt, J. Phys. Chem. B **109** 6422 (2005).
6. H. E. Stanley, P. Kumar, L. Xu, Z. Yan, M. G. Mazza, S. V. Buldyrev, S. -H. Chen and F. Mallamace, Physica A **386** 729 (2007).
7. N. Giovambattista, P. G. Debenedetti, C. F. Lopez, and P. J. Rossky, Proc. Natl. Acad. Sci. U.S.A **105** 2274 (2008).

8. P. G. Debenedetti, Metastable Liquids, Priceton University Press, Priceton, NJ (1996).
9. O. Mishima and H. E. Stanley, Nature **396** 329 (1998).
10. C. A. Angell, Chem. Rev. **102** 2627 (2002).
11. C. A. Angell, Annu Rev. Phys. Chem. **55** 559 (2004).
12. D. C. Malaspina, E. P. Schulz, L. M. Alarcón, M. A. Frechero and G. A. Appignanesi, Eur. Phys. J. E **32** 35 (2010).
13. E. Shiratani and M. Sasai, J. Chem. Phys. **104** 7671 (1996).
14. E. Shiratani and M. Sasai, J. Chem. Phys. **108**, 3264 (1998).
15. M. Sasai, Physica A **285** 315 (2000).
16. M. Sasai, J. Chem. Phys. **118** 10651 (2003).
17. H. Tanaka, Phys. Rev. Lett. **80** 5750 (1998).
18. H. Tanaka, Europhys. Lett. **50** 340 (2000).
19. H. Tanaka, J. Chem. Phys. **112** 799 (2000).
20. G. A. Appignanesi, J. A. Rodriguez Fris and F. Sciortino, Eur. Phys. J. E **29** 305 (2009).
21. O. Mishima, L. D. Calvert and E. Whalley, Nature **310**, 393 (1984).
22. H.-G. Heide, Ultramicroscopy **14** 271 (1984).
23. P.-L. Chau and A. J. Hardwick, Mol. Phys. **93** 511 (1998).
24. J. R. Errington and P. G. Debenedetti, Nature **409** 318 (2001).
25. I. Naberukhin Yu, V. P. Voloshin and N. N. Medvedev, Mol. Phys. **73** 917 (1991).
26. A. Oleinikova and I. Brovchenko, J. Phys.: Condensed Matter **18** S2247 (2006).
27. S. R. Accordino, J. A. Rodriguez Fris, F. Sciortino and G. A. Appignanesi, Eur. Phys. J. E **34** 48 (2011).
28. J. Gelman Constantin, A. Rodriguez Fris, G. Appignanesi, M. Carignano, I. Szleifer and H. Corti, Eur. Phys. J. E **34** 126 (2011).
29. K. T. Wikfeldt, A. Nilsson and L. G. M. Pettersson, Phys. Chem. Chem. Phys. **13** 19918 (2011).
30. J. Zielkiewicz J. Chem. Phys. **123** 104501 (2005).
31. B. Santraa, R. A. DiStasio Jr., F. Martellia and R. Car Mol. Phys. **113** 2829 (2015).
32. J. A. Rodriguez Fris, G. A. Appignanesi, E. La Nave and F. Sciortino, Phys. Rev. E **75** 041501 (2007).
33. G. A. Appignanesi, J. A. Rodriguez Fris, R. A. Montani and W Kob, Phys. Rev. Lett. **96** 057801 (2006)
34. G. A. Appignanesi and J. A. Rodriguez Fris J. Phys.: Condens. Matter **21** 203103 (2009)
35. R. A. L. Valleé, W. Paul, and K. Binder, J. Chem. Phys. **127** 154903 (2007).
36. J. A. Rodriguez Fris, G. A. Appignanesi and E. R. Weeks, Phys. Rev. Lett. **107** 065704 (2011)
37. H. J. C. Berendsen, J. R. Grigera and T. P. Stroatsma, J. Phys. Chem. **91** 6269 (1987).
38. S. Rick, J. Chem. Phys. **120** 6085 (2004).
39. P. G. Debenedetti and F. H. Stillinger, Nature **410** 259 (2001).
40. R G Fernandez, J L. F. Abascal and C Vega, J. Chem. Phys. **124** 144506 (2006).
41. J. Russo and H. Tanaka, Nature Communications **5**, 3556 (2014).
42. C. H. Cho, S. Singh, and G. W. Robinson, Phys. Rev. Lett. 76, 1651 (1996)
43. J. Urquidi, S. Singh, C. H. Cho, and G. W. Robinson, Phys. Rev. Lett. **83** 2348 (1999).
44. E. G. Ponyatovsky, V. V. Sinitsyn, and T. A. Pozdnyakova, JETP Lett. **60** 360 (1994).
45. E. G. Ponyatovsky, V. V. Sinitsyn, and T. A. Pozdnyakova, J. Chem. Phys. **109** 2413 (1998).
46. E. G. Ponyatovsky, J. Phys.: Condens. Matter **15** 6123 (2003).
47. Sciortino, F., Geiger, A. and Stanley, H. E. Phys. Rev. Lett.65, 3452 (1990)
48. F. Sciortino, A. Geiger and H. E. Stanley, Phys. Rev. Lett. **65** 3452 (1990).
49. C. Donati, J. F. Douglas, W. Kob, S. J. Plimpton, P. H. Poole and S. C. Glotzer, Phys. Rev. Lett. **80**, 2338 (1998).
50. M. D. Ediger, C. A. Angell and S. R. Nagel, J. Phys.Chem. B 100, 13 200 (1996).
51. E. R. Weeks, J. C. Crocker, A.C. Levitt, A. Schofield and D. A. Weitz, Science 287, 627 (2000).
52. G. A. Appignanesi, J. A. Rodriguez Fris, and M.A. Frechero, Phys. Rev. Lett. **96** 237803 (2006).
53. A. Widmer-Cooper, P. Harrowell and H. Fynewever, Phys. Rev. Lett. **93**, 135701 (2004).
54. G. S. Matharoo, M. S. G. Razul and P. H. Poole, Phys. Rev. E **74**, 050502 (2006).
55. L. O. Hedges and J. P. Garrahan, J. Phys.: Condensed Matter **19**, 205124 (2007).
56. B. Doliwa and A. Heuer, Phys. Rev. Lett. **91**, 235501 (2003).
57. C. P. Royall, S. R. Williams, T. Ohtsuka and H. Tanaka, Nature Materials **7**, 556 - 561 (2008).
58. I. Ohmine, J. Phys. Chem. **99**, 6765 (1995).
59. D. Schlesinger et al., The Journal of Chemical Physics **145**, 084503 (2016).